

AD-A052 781

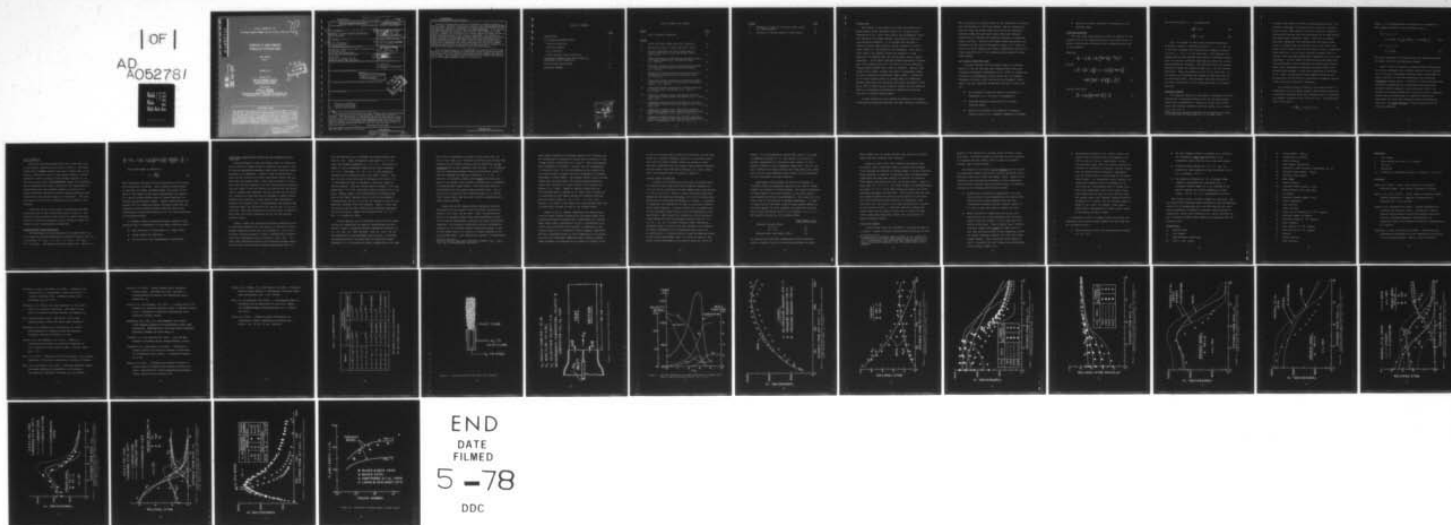
AERONAUTICAL RESEARCH ASSOCIATES OF PRINCETON INC N J F/G 21/2
PROPERTIES OF LARGE TURBULENT HYDROGEN/AIR DIFFUSION FLAMES.(U)
OCT 77 H S PERGAMENT, E S FISHBURNE F33657-77-C-0437

UNCLASSIFIED

ARAP-316-PT-1

NL

| OF |
AD
A052781



AD A 052781

A.R.A.P. REPORT NO. 316

AIR FORCE CONTRACT NUMBER F33657-77-C-0437, ITEM 0004

1
3

PROPERTIES OF LARGE TURBULENT
HYDROGEN/AIR DIFFUSION FLAMES

FINAL REPORT

PART 1

OCTOBER 1977

Prepared For

FOREIGN TECHNOLOGY DIVISION
AIR FORCE SYSTEMS COMMAND
UNITED STATES AIR FORCE

Prepared By

HAROLD S. PERGAMENT
E. STOKES FISHBURNE

AERONAUTICAL RESEARCH ASSOCIATES OF PRINCETON, INC.
50 WASHINGTON ROAD, PRINCETON, NEW JERSEY 08540

DDC
APR 18 1978
F

AD No.
DDC FILE COPY

DISCLAIMER CLAUSE

This document was prepared for the Air Force Systems Command by a U.S. contractor. Conclusions/views contained therein are based on analysis of such information as could be made available to the contractor under the terms of the contract and appropriate security directives. It has been reviewed by Foreign Technology Division, AFSC, but does not necessarily represent an approved Department of Defense position and is not to be considered a Department of Defense Intelligence Product.

This document has been approved
for public release and sale; its
distribution is unlimited.

UNCLASSIFIED

SECURITY CLASSIFICATION OF THIS PAGE (When Data Entered)

ARAP-316-PT-1

REPORT DOCUMENTATION PAGE		READ INSTRUCTIONS BEFORE COMPLETING FORM
1. REPORT NUMBER	2. GOVT ACCESSION NO.	3. RECIPIENT'S CATALOG NUMBER
4. TITLE (and Subtitle) PROPERTIES OF LARGE TURBULENT HYDROGEN/AIR DIFFUSION FLAMES.	5. TYPE OF REPORT & PERIOD COVERED Final Report (Part 1), 9 May 77 - 30 Sep 77	6. PERFORMING ORG. REPORT NUMBER A.R.A.P. Report No. 316 (Part 1)
7. AUTHOR(s) Harold S. Pergament E. Stokes Fishburne	8. CONTRACT OR GRANT NUMBER(s) F33657-77-C-0437 Item 0004	9. PROGRAM ELEMENT, PROJECT, TASK AREA & WORK UNIT NUMBER 444P1
9. PERFORMING ORGANIZATION NAME AND ADDRESS Aeronautical Research Associates of Princeton, Inc. 50 Washington Road Princeton, New Jersey 08540	10. CONTROLLING OFFICE NAME AND ADDRESS USAF, AFSC Aeronautical Systems Division Wright-Patterson AFB, Ohio 45433	11. REPORT DATE Oct 77
11. CONTROLLING OFFICE NAME AND ADDRESS USAF, AFSC Aeronautical Systems Division Wright-Patterson AFB, Ohio 45433	12. NUMBER OF PAGES 38	13. SECURITY CLASS. (of this report) Unclassified
14. MONITORING AGENCY NAME & ADDRESS (if different from Controlling Office)	15. SECURITY CLASS. (of this report) Unclassified	15a. DECLASSIFICATION/DOWNGRADING SCHEDULE
16. DISTRIBUTION STATEMENT (of this Report) <div style="border: 1px solid black; padding: 5px; display: inline-block;">This document has been approved for public release and sale; its distribution is unlimited.</div>		
17. DISTRIBUTION STATEMENT (of the abstract entered in Block 20, if different from Report)		
18. SUPPLEMENTARY NOTES		
19. KEY WORDS (Continue on reverse side if necessary and identify by block number) hydrogen/air combustion buoyant diffusion flames turbulent reacting flows		
20. ABSTRACT (Continue on reverse side if necessary and identify by block number) The prediction of IR radiation from large, turbulent H ₂ /air diffusion flames requires a detailed analysis of flame properties, including the effects of buoyancy. This report gives the methodology employed for analyzing such flames and the results of calculations on large flames, including those from the North American Rockwell C-1 stack. These (and subsequent) results have been used as input to the IR radiation calculations on the C-1 stack discussed in Part 2 of this final report. → next page (Continued on next page)		

UNCLASSIFIED

1 SECURITY CLASSIFICATION OF THIS PAGE (When Data Entered)

DD8 4000

See

UNCLASSIFIED

SECURITY CLASSIFICATION OF THIS PAGE(When Data Entered)

The model discussed herein treats the axisymmetric turbulent mixing of co-flowing streams, including nonequilibrium chemistry, employing ^{an} the Donaldson/Gray eddy viscosity formulation. Comparisons are made between model predictions and the nonbuoyant laboratory H₂/air flame data of Kent and Bilger. It is shown that centerline temperatures and species mole fractions can be predicted to good accuracy. However, the calculated rate of radial transport of energy and mass is greater than that measured in the laboratory experiments. The results of a series of parametric calculations on buoyant flames and comparisons with buoyant flame length data show that: (1) flame properties scale with nondimensional distance for Froude numbers (Fr) greater than about 10⁶, (2) buoyancy significantly affects temperature decay rates downstream of the location of maximum temperature (after all the H₂ has burned), and (3) the predicted influence of Fr on buoyant flame lengths is consistent with the available data. ←

1,000,000

From the above analysis it is concluded that the predicted C-1 stack flame widths are too narrow, although the flame heights should be reasonably accurate. This should result in IR radiation predictions which are somewhat less than the actual values. This conclusion has been verified by the radiation measurements on C-1 stack flames presented in Part 2 of this report.

TABLE OF CONTENTS

	<u>PAGE</u>
INTRODUCTION	1
GAS DYNAMICS/CHEMISTRY MODEL	2
Governing Equations	3
Turbulence Models	4
H ₂ /O ₂ Chemistry	7
Scaling Buoyant Flame Properties	7
COMPARISONS BETWEEN MODEL PREDICTIONS AND LABORATORY H ₂ /AIR FLAME DATA	9
BUOYANT FLAME CALCULATIONS	13
CONCLUDING REMARKS	15

ACCESSION for	
NTIS	White Section <input checked="" type="checkbox"/>
DDC	Buff Section <input type="checkbox"/>
UNANNOUNCED	<input type="checkbox"/>
JUSTIFICATION <i>on file</i>	
BY	
DISTRIBUTION/AVAILABILITY CODES	
Dist	SP CIAL
<i>A</i>	

LIST OF TABLES AND FIGURES

<u>TABLE</u>		<u>PAGE</u>
1	H ₂ /O ₂ Combustion Reactions	24
 <u>FIGURE</u>		
1	H ₂ /air diffusion flame with pilot ignition.	25
2	Experimental setup of Kent and Bilger (1973).	26
3	Initial conditions for model predictions to compare with data of Kent and Bilger (1973); x/r _j = 12.2 .	27
4	Comparison between predicted and measured center-line temperatures-H ₂ /air laboratory flame, r _j = 0.38 cm .	28
5	Comparison between predicted and measured center-line mole fractions-H ₂ /air laboratory flame, r _j = 0.38 cm .	29
6	Comparison between predicted and measured radial temperature profiles-H ₂ /air laboratory flame, r _j = 0.38 cm .	30
7	Comparison between predicted and measured radial nitrogen mole fraction profiles-H ₂ /air laboratory flame, r _j = 0.38 cm .	31
8a	Comparison between temperature profiles predicted by present model and Rhodes et al. (1974); x/r _j = 160 .	32
8b	Comparison between radial temperature profiles predicted by present model and Rhodes et al. (1974); x/r _j = 320 .	33
9	Comparison between radial mole fraction profiles predicted by present model and Rhodes et al. (1974); x/r _j = 160 .	34
10	Comparison between radial temperature profiles predicted by present model and second-order closure model of Fishburne et al. (1977); x/r _j = 80 .	35
11	Comparison between radial mole fraction profiles predicted by present model and second-order closure model of Fishburne et al. (1977); x/r _j = 80 .	36

FIGURE

PAGE

- | | |
|----|---|
| 12 | Influence of buoyancy on H_2 /air flame center-line temperatures. |
| 13 | Influence of Froude number on flame length. |

37

38

INTRODUCTION

The purpose of this paper is to study the properties of large buoyant H_2 /air diffusion flames via a computer model (Mikatarian et al., 1972) which treats the axisymmetric turbulent mixing of co-flowing streams, including the effects of nonequilibrium chemistry. It is assumed that hydrogen is "vented" through large vertical stacks, ignited via a pilot flame (Figure 1), and burned in the atmosphere. This type of flame exists, for example, during the disposal of large quantities of hydrogen used for testing space shuttle engine components. At the North American Rockwell/Rocketdyne Division, mass flows ranging from 10 to 150 lb/sec of H_2 are exhausted through stacks greater than 2 feet in diameter. Because these flames are so large, buoyancy will have a considerable effect on their properties, particularly flame lengths. Calibration of the above computer model is accomplished via comparisons between predictions and laboratory data (Kent and Bilger, 1973; Kent, 1972) on small H_2 /air diffusion flames, and the predicted effects of buoyancy are evaluated by comparing calculations with data on buoyant flame lengths.

In what follows we first discuss the details of the model, including the governing equations, the eddy viscosity formulation,

and the results of a recent review of the literature on reaction rate coefficients for the H_2/O_2 system. Next we compare predictions using the present model with the H_2 /air laboratory diffusion flame data and other models which use different formulations to describe the turbulent transport of momentum, energy, and mass. Finally, the buoyant flame calculations are presented and the results discussed in terms of (1) those conditions for which buoyancy will have a significant influence on flame properties and (2) the comparison with measured buoyant flame lengths.

GAS DYNAMICS/CHEMISTRY MODEL

The model utilized for the present study is a modified version of the Low Altitude Plume Program (LAPP) which was originally developed by Mikatarian et al. (1972) to compute the properties of afterburning rocket plumes; see, for example, Pergament and Jensen (1971) and Jensen and Pergament (1971). Some of the more important assumptions employed in this model are:

- The influence of external winds on the flame is negligible, i.e., the flow is axisymmetric.
- Turbulent mixing is characterized by an eddy viscosity model.
- There is no influence of turbulence on chemical reaction rates, i.e., "laminar" chemistry is assumed.

- There is no direct influence of turbulence on the buoyancy terms.

Governing Equations

The free shear layer equations, with the addition of the buoyancy term in the momentum equation, are written below in stream function-type coordinates (the coordinate system used in the program).

Momentum:

$$\frac{\partial u}{\partial x} = -\frac{1}{\rho u} \frac{dp}{dx} + \frac{1}{\Psi} \frac{\partial}{\partial \Psi} \left[\frac{\mu \rho u r^2}{\Psi} \frac{\partial u}{\partial \Psi} \right] + \frac{g(\rho_e - \rho)}{\rho u} \quad (1)$$

Energy:

$$\begin{aligned} c_p \frac{\partial T}{\partial x} = & \frac{1}{\rho} \frac{dp}{dx} - \frac{1}{\rho u} \sum_1 h_1 \dot{w}_1 + \frac{1}{\Psi} \frac{\partial}{\partial \Psi} \left[\frac{c_p}{Pr} \frac{\mu \rho u r^2}{\Psi} \frac{\partial T}{\partial \Psi} \right] \\ & + \frac{\mu \rho u r^2}{\Psi^2} \left[\left(\frac{\partial u}{\partial \Psi} \right)^2 + \frac{Le}{Pr} \frac{\partial T}{\partial \Psi} \sum_1 c_{p1} \frac{\partial F_1}{\partial \Psi} \right] \end{aligned} \quad (2)$$

Species Continuity:

$$\frac{\partial F_1}{\partial x} = \frac{1}{\Psi} \frac{\partial}{\partial \Psi} \left[\left(\frac{Le}{Pr} \right) \frac{\mu \rho u r^2}{\Psi} \frac{\partial F_1}{\partial \Psi} \right] + \frac{\dot{w}_1}{\rho u} \quad (3)$$

The stream function, Ψ , is defined by*

$$\Psi \frac{\partial \Psi}{\partial r} = \rho u r \quad (4a)$$

$$\Psi \frac{\partial \Psi}{\partial x} = - \rho v r \quad (4b)$$

Eqs. (1) through (4) are solved via finite-difference techniques, subject to specified values of u , T , and F_1 at the outer boundary (free stream) and a symmetry condition ($\partial u / \partial \Psi = 0$, etc.) on the flame axis. Both momentum and energy equations are handled by an explicit difference scheme, while the species continuity equations are solved via a mixed implicit/explicit technique. The diffusion terms are treated explicitly, while the chemistry terms (i.e., \dot{w}_1) are treated implicitly. Thus, the solution to Eq. (3) at each step, Δx , is obtained by linearizing the chemistry terms and inverting the resulting matrix. The diffusion terms then form part of the known column matrix on the right-hand side of the matrix equation.

Turbulence Models

It is not our purpose in this paper to determine the "best" description of turbulent mixing to use for the large buoyant flames under consideration. Suffice it to say that we have chosen the simplest formulation for this study, i.e., an eddy

*Note that this definition results in a stream function which is proportional to the square root of the mass flow.

viscosity model based on Prandtl's mixing length theory. The potential advantages of using one or two equation turbulent kinetic energy (TKE) models to describe turbulent transport in nonreacting flows has been fully discussed in the NASA/Langley Free Shear Layer Conference (1973). There are no similar published comparisons for reacting flows with large energy release, although data are available (e.g., Kent (1972) and Rhodes (1977)) which could form the basis for such a comparison. These data have, in fact, been utilized by Rhodes (1977) to initiate such turbulent mixing model comparisons for flows with combustion. In this regard it should also be mentioned that the second-order closure techniques for describing turbulent shear flows, developed by Donaldson and Varma (1976), have recently been extended to flows with combustion by Fishburne et al. (1977) including multi-step chemical reactions and incorporation of the effect of turbulence on chemical reaction rates (so-called "turbulent" chemistry).

The turbulence model utilized in the present study is a modification of the original Prandtl eddy viscosity model due to Donaldson and Gray (1966) who correlated data on supersonic and subsonic nonreactive jets into still air. The expression used in the code is

$$\mu = \frac{K}{2} (r_{1/2} - r_1) \rho |u_o - u_e| \quad (5)$$

where K (a "compressibility" correction) is a function of Mach number evaluated at the half-radius ($M_{1/2}$).

For $M_{1/2} \leq 1.2$:

$$K = 0.0468 + M_{1/2} \left(-0.046 M_{1/2} + 0.0256 M_{1/2}^2 \right) \quad (6a)$$

For $M_{1/2} > 1.2$:

$$K = 0.0248 \quad (6b)$$

The above expression is consistent with the observed decrease in mixing rate with increasing Mach number.

Smoot (1976) has recently correlated mixing coefficients for coaxial submerged (zero external velocity) and co-flowing jets — and has, by analyzing additional data, reconfirmed the overall validity of the above expressions for predicting centerline velocity decay. In addition, he has correlated some nonreactive temperature and concentration data and shows turbulent Prandtl numbers to vary from about 0.85 to 1.0. However, as we shall demonstrate in the next section, agreement between data and predictions of centerline velocity and temperature for flows with combustion does not necessarily imply that the radial profiles of these properties will be correctly predicted.

H₂/O₂ Chemistry

The H₂/O₂ reaction mechanism and rate coefficients used in the present calculations are given in Table I. The rates listed under "PRESENT VALUES" were used to obtain most of the results. During the course of this study, however, a recent literature survey by Kurzius (1975) became available to us. The rates listed under "NEW RECOMMENDED VALUES" are essentially those recommended by Kurzius, except that the three-body rate coefficients have been modified slightly to account for a single third-body efficiency (Kurzius assigned different efficiencies for each species acting as a third body). The original sources for the rate coefficient data are given in the Appendix.

During the course of this study, calculations were made using both sets of rate coefficients given in Table I. The resulting flame properties were found to be nearly identical, primarily because one-atmosphere H₂/air diffusion flames are nearly in local thermochemical equilibrium.

Scaling Buoyant Flame Properties

The appropriate scaling parameters for buoyant flames can be obtained by nondimensionalizing the momentum equation (Eq.(1)). If we define $\bar{x} = x/d_j$, $\bar{u} = u/u_j$, $\bar{r} = r/d_j$, $\bar{\rho} = \rho/\rho_j$, $\bar{\psi}^2 = \psi^2/\rho_j u_j r_j^2$, the momentum equation becomes (for $dp/dx = 0$):

$$\frac{\partial \bar{u}}{\partial \bar{x}} = K(\bar{r}_{1/2} - \bar{r}_1)(\bar{u}_o - \bar{u}_e) \frac{1}{\bar{\psi}} \frac{\partial}{\partial \bar{\psi}} \left[\bar{\rho}^2 \bar{u} \bar{r}^2 \frac{1}{\bar{\psi}} \frac{\partial \bar{u}}{\partial \bar{\psi}} \right] + \frac{g d_j}{u_j^2} \left[\frac{1}{\bar{u}} \left(\frac{\bar{\rho}_e}{\bar{\rho}} - 1 \right) \right] \quad (7)$$

The Froude number is defined as

$$Fr = \frac{u_j^2 / d_j}{g} \quad (8)$$

which represents the ratio of the acceleration of the fluid to the acceleration of gravity. Thus, buoyancy effects should be important for large, low-speed flames (low values of Fr). Later in this paper we will show quantitatively the values of Fr at which buoyancy effects start to become important for vertical H_2 /air diffusion flames. Similar normalizations are possible for the energy and species continuity equations, but scaling can only be achieved under conditions where local thermochemical equilibrium prevails; i.e., the flame properties are mixing-controlled.

In summary, suitably normalized buoyant turbulent flame properties will be independent of size under conditions where:

- Eddy viscosity is proportional to a length scale.
- Froude numbers are identical.
- The flow is in local thermochemical equilibrium.

COMPARISONS BETWEEN MODEL PREDICTIONS AND LABORATORY H₂/AIR FLAME DATA

The measurements of Kent and Bilger (1973) on laboratory H₂/air diffusion flames provide an excellent data base to test the present gasdynamics/chemistry model under conditions where buoyancy is not important. Figure 2 shows the experimental setup and the conditions of those tests whose results are compared with the present model. This setup resulted in a favorable axial pressure gradient; the free stream velocity variation over the length of the test section is given by Kent and Bilger (1973), together with measured velocity profiles at the nozzle lip. Because the LAPP code was not designed to handle initial boundary layer profiles, a code, based on that developed by Patankar and Spalding (1967), incorporating a two equation TKE turbulence model was utilized for the initial part of the calculations. This code generated the profiles given in Figure 3, which were the initial conditions for all the calculations reported herein.

Figure 4 shows that predicted centerline temperatures are in reasonable agreement with the data up to the point of near-maximum temperature (data were only obtained to $x/r_j \approx 320$). The axial pressure gradient is seen to significantly influence centerline temperatures only at values of $x/r_j > 240$. At these large downstream distances the difference between centerline and free stream velocity becomes sufficiently small for

the accelerating flow to influence the overall mixing rate (see Eq. (5)). These calculations were made for $Pr = 0.7$ (with the standard assumption of $Le = 1.0$). Also shown in Figure 4 (and in subsequent figures) are results assuming $Pr = 1.0$; the range $0.7 < Pr < 1.0$ is that generally reported in the literature (see, e.g., Smoot (1976)). From Eqs. (2) and (3) we note that an increase in Pr from 0.7 to 1.0 decreases the rate of transport of mass and energy by similar amounts. From the results shown in Figure 4, it would appear that $Pr \approx 0.85$ would give nearly a perfect fit to the data. However, there is no justification for assuming that this is the "best" constant value to use for the complete flowfield, and, in fact, it is not our purpose to back out any empirical constants from this analysis. Figure 5 shows that the axial H_2 and H_2O mole fractions are predicted reasonably well by the theory. Again, the predictions for $Pr = 0.7$ and 1.0 bracket the data.

A more rigorous test of the theory is how well the radial profiles of temperature and species concentrations are predicted. Figure 6 compares predicted temperature profiles for $Pr = 0.7$ and 1.0 with the data. Only for $x/r_j = 80$ are the predictions in good agreement with the data. At farther downstream stations, the flame width is drastically underestimated, i.e., the predicted overall mixing rate is too high.

This point is emphasized in Figure 7 which shows that, for most of the flame, N_2 is predicted to diffuse more rapidly than indicated by the data*, although, again, predictions on the centerline are in good agreement with the data. It is apparent that the discrepancy between theory and experiment cannot be fixed by changing the empirical constants K or Pr . A variation in turbulent length scales across the flame would appear to be needed, with possibly a varying ratio of momentum to energy/species length scales. This obviously cannot be accomplished with the present eddy viscosity model. Use of the one or two equation TKE turbulence models, or a second-order closure model, may well give a better representation of these radial profiles.

Figures 8a and 8b compare radial temperature profiles calculated with the present theory with those calculated by Rhodes et al. (1974) and the data. Their calculations are based on an integral (rather than finite-difference) method for solving the differential equations and assume equilibrium chemistry. The turbulent mixing model solves a differential equation for the turbulent kinetic energy and assumes a form for the length scale as a function of radial distance (a one equation TKE model). The authors also describe a "fluctuating"

* N_2 mole fraction data were obtained by summing X_{H_2} , X_{H_2O} , and X_{O_2} and subtracting from unity.

model which formulates the average density as an "average over the instantaneous concentration groups which contribute to the average element concentration at a point." This "fluctuating" model represents an attempt to account for the "unmixedness" of turbulent flows. No firm conclusions can be reached from the results shown in Figures 8a and 8b regarding the relative advantages of these models. The present theory, using a mixing length eddy viscosity model with nonequilibrium chemistry, agrees with these data at least as well as the theories of Rhodes et al. (1974). Figure 9, however, shows that the "fluctuating" model of Rhodes et al. (1974) does a better job of accounting for the radial species mole fraction profiles than the present model at $x/r_j = 160$. At $x/r_j = 320$, however, (not shown in this paper) the "fluctuating" model does not agree with the data as well as the "steady" model.

Figures 10 and 11 compare temperature and species mole fraction radial profiles predicted by the present model with predictions using the second-order closure model for reacting shear layers (RSL), developed at A.R.A.P. by Fishburne et al. (1977), with and without the influence of turbulence on the reaction rates (i.e., "turbulent" versus "laminar" chemistry). The most interesting result of these comparisons is a qualitative one; the "turbulent" chemistry model predicts a nonzero flame thickness (as indicated by the amount of overlap of the

H₂ and O₂ profiles) which is more in accord with the data than either the "laminar" chemistry results or the present model. The latter two models predict almost no overlap in these profiles, consistent with the classic "flame sheet" assumption. Similar results were obtained by Rhodes et al. (1974) using their "fluctuating" model (as shown in Figure 9).

BUOYANT FLAME CALCULATIONS

A series of calculations was made with the present model for vertical stack flames with exit diameters ranging from 0.5 cm to 68 cm, resulting in Froude numbers which vary between 9×10^6 to 3.5×10^4 . Figure 12 shows calculated centerline temperature distributions (assuming $Pr = 0.7$) for three model stacks and the North American Rockwell C-1 stack. If buoyancy is neglected, the temperature is seen to scale with nondimensional axial distance. As noted earlier this is expected for one atm turbulent H₂/air flames, since the chemistry is near-equilibrium. When buoyancy is included in the calculations, slight departures from the universal profile occur at $Fr = 9 \times 10^5$. As Fr is further reduced, rather substantial departures from the scaled curve are observed — but primarily in regions downstream of the temperature peak, where the acceleration due to buoyancy starts to have an important effect on the overall entrainment rate. As noted in Figure 12 this effect occurs downstream of the location where all the H₂ is

burned. It is interesting to observe that, while a two order of magnitude increase in Fr only shifts the location of maximum temperature by a relatively small amount, it has a drastic influence on the temperature decay rate. This in turn will influence the radial profiles and flame widths (not shown here) and will have important implications for the prediction of such observables as flame radiation.

Experimental data showing the effects of buoyancy on diffusion flames are generally reported in the form of "flame length" as a function of Froude number. One typical definition of flame length is the axial distance to the point having a mean composition which is stoichiometric. This turns out to be quite close to the position of maximum temperature. In order to judge how well the model predicts flame lengths defined in the above manner, we first compared our predictions with the data of Kent and Bilger (1973) for no buoyancy, i.e., $Fr \rightarrow \infty$. The results are given in the following table:

	<u>FLAME LENGTH, L_f/d_j</u>
Predicted (Present Model)	
$Pr = 1.0$	167
$Pr = 0.7$	110
Measured (Kent and Bilger (1973))	135

As expected from the axial temperatures and mole fractions shown in Figures 4 and 5, the predictions bracket the data.

These lengths are, of course, greater than those for diffusion flames with zero external (air) velocity.

Bilger and Beck (1974) have compiled experimental data from Baker (1972), Hawthorne (1949), and Lavoie and Schlader (1973) showing the influence of Froude number on H_2 /air diffusion flame lengths*, in addition to reporting their own measurements. Comparisons have been made (Figure 13) between the measured flame lengths and predictions from the present model. Figure 13 shows that, for $Pr = 0.7$, the flame lengths are underpredicted; but using $Pr = 1.0$ in the model brings the theory into quite reasonable agreement with the data. These results indicate that the buoyancy effects are correctly accounted for by the model, even though predicted radial profiles of temperature, mole fractions, etc. are subject to the same uncertainties discussed in the previous section. A detailed comparison between the present model and the radial profile data of Bilger and Beck (1974) should give additional insight into the analysis of buoyant diffusion flames.

CONCLUDING REMARKS

A model which treats the axisymmetric turbulent mixing of co-flowing streams, including nonequilibrium chemistry, has been

*A translation of a Russian paper by Bayev et al. (1974) also contains H_2 /air diffusion flame length data as a function of Fr . Unfortunately, the data have been normalized in such a manner that ready comparisons with the present model are not possible.

applied to the prediction of buoyant H_2 /air diffusion flame properties. Turbulent mixing is described via the formulation of Donaldson and Gray (1966), which is based on Prandtl's original eddy viscosity model.

The adequacy of the model for no buoyancy has been tested by comparisons between calculations and the laboratory H_2 /air diffusion flame data of Kent and Bilger (1973). Based on this comparison, and calculations performed by other researchers using different computer models and descriptions of turbulent transport, the following observations are made:

- Predictions of centerline temperatures (up to the axial location of peak temperature) and species mole fractions are in good agreement with the data. Calculations assuming turbulent Prandtl numbers of 0.7 and 1.0 have been shown to bracket the data.
- Radial profiles of temperature and species mole fractions are not in good agreement with the data; radial turbulent transport is less rapid than predicted by the model. This indicates that a constant turbulent length scale across the flame (used in most eddy viscosity models) cannot adequately account for radial turbulent transport for flows with large energy release. (This conclusion should apply as well to internal flows with combustion, afterburning rocket exhaust plumes, etc.)

- Calculations by Rhodes et al. (1974), using a one equation TKE turbulence model and Fishburne et al. (1977) using the A.R.A.P. second-order closure reacting shear layer (RSL) code (which includes the influence of turbulence on chemical reaction rates) have not demonstrated a substantial improvement over the present model in accounting for the radial profile data. In a qualitative sense, however, the "turbulent" chemistry model of Fishburne et al. (1977) and the "fluctuating" model of Rhodes et al. (1974) are improvements since both predict flame zone widths that are more in accord with the data. The present model, the "laminar" chemistry model of Fishburne et al. (1977), and the "steady" model of Rhodes et al. (1974) all predict a very narrow flame width — approaching the "flame sheet" common in describing diffusion flames.

A parametric series of buoyant flame calculations and comparisons with measured flame lengths have been made with the following results:

- Flame properties scale with nondimensional distance for $Fr > 10^6$.

- The most dramatic effect of buoyancy is to influence the temperature decay rate downstream of the temperature peak, after all the H_2 has been burned.
- Predicted flame lengths for $Pr = 0.7$ and 1.0 bracket the value measured by Kent and Bilger (1973) for no buoyancy, $Fr \rightarrow \infty$.
- The predicted influence of Fr on buoyant flame lengths is consistent with available data. A turbulent Prandtl number of 1.0 is required in the model to predict the correct magnitude of flame length. Use of $Pr = 0.7$ underpredicts the data.

This study of H_2 /air diffusion flames is continuing. The two equation TKE turbulence model developed by Rodi and Spalding (1970) will be incorporated into the LAPP code and the calculations repeated to determine if measured radial profiles of temperature, species mole fractions, etc. can be accounted for and if predicted buoyant flame lengths are consistent with the available data.

NOMENCLATURE

c_p	specific heat
d_j	jet diameter
D	eddy diffusion coefficient
F_1	X_1/W ; also Y_1/W_1

Fr	Froude number, $u_j^2/d_j g$
g	acceleration of gravity
h	static enthalpy
k	eddy thermal conductivity
K	constant in eddy viscosity formulation, Eq. (5)
Le	turbulent Lewis number, $\rho D c_p / k$
L_f	diffusion flame length
M	Mach number
p	static pressure
Pr	turbulent Prandtl number, $\mu c_p / k$
r	radial distance from flame axis
r_j	jet radius
Sc	turbulent Schmidt number, $\mu / \rho D$
T	static temperature
u	axial velocity
v	normal velocity
\dot{w}_i	molar rate of production of i^{th} species
W	molecular weight of mixture
W_i	molecular weight of i^{th} species
x	axial distance
X_i	mole fraction of i^{th} species
Y_i	mass fraction of i^{th} species
ρ	density
Ψ	stream function
μ	eddy viscosity

Subscripts

- e free stream
i inner mixing zone; also i^{th} species
j jet exit
o centerline
 $1/2$ evaluated at half-width; value of r where $u = (u_o + u_e)/2$

REFERENCES

- Baker, D.J. (1972). Nitric oxide formation in turbulent diffusion flames. B.E. thesis, University of Sydney.
- Bayev, V.K., et al. (1974). On the length of diffusion flames. (Russian Translation). *Physics of Combustion and Explosion*, No. 4, pp. 485-492.
- Bilger, R.W., and Beck, R.E. (1974). Further experiments on turbulent jet diffusion flames. University of Sydney, Charles Kolling Research Laboratory Technical Note F-67. See also, *Fifteenth Symposium (International) on Combustion* (1975), The Combustion Institute, Pittsburgh, PA, pp. 541-553.
- Donaldson, C. duP., and Gray, K.E. (1966). Theoretical and experimental investigation of the compressible free mixing of two dissimilar gases. *AIAA J.*, 4, pp. 2017-2025.

- Donaldson, C. duP., and Varma, A.K. (1976) . Remarks on the construction of a second-order closure description of turbulent reacting flows. *Combustion Science and Technology*, 13, pp. 55-78.
- Fishburne, E.S., Varma, A.K., and Donaldson, C. duP. (1977) . Aspects of turbulent combustion. *AIAA Paper 77-100*, AIAA 15th Aerospace Sciences Meeting, Los Angeles, CA.
- Free turbulent shear flows. *NASA SP-321* (1973), NASA Langley Research Center Free Shear Layer Conference.
- Hawthorne, W.R., Weddell, D.S., and Hottel, H.C. (1949) . *Third Symposium of Combustion Flame and Explosion Phenomena*, Williams and Wilkins, p. 266.
- Jensen, D.E., and Pergament, H.S. (1971) . Effects of nonequilibrium chemistry on electrical properties of solid propellant rocket exhaust plumes. *Combust. Flame*, 12, p. 115.
- Kent, J.H. (1972) . Turbulent jet diffusion flames. Ph.D. thesis, Department of Mechanical Engineering, University of Sydney.
- Kent, J.H., and Bilger, R.W. (1973) . Turbulent diffusion flames. *Fourteenth Symposium (International) on Combustion*, The Combustion Institute, Pittsburg, PA, pp. 615-625.

- Kurzius, S.C. (1975). Rocket exhaust global combustion reaction model. *LMSC-HREC TR-511027*, Appendix A, Lockheed-Huntsville Research and Engineering Center, Huntsville, AL.
- Lavoie, G.A., and Schlader, A.F. (1973). A scaling study of NO formation in turbulent diffusion flames of hydrogen burning in air. Department of Mechanical Engineering, Laval University, Quebec, Canada.
- Mikatarian, R.R., Kau, C.J., and Pergament, H.S. (1972). A fast computer program for nonequilibrium rocket plume predictions. *AFRPL-TR-72-94*, Air Force Rocket Propulsion Laboratory, Edwards Air Force Base, CA.
- Patankar, S.V., and Spalding D.B. (1967). *Heat and Mass Transfer in Boundary Layers*, Morgan-Grampian, London.
- Pergament, H.S., and Jensen, D.E. (1971). Influence of chemical kinetic and turbulent transport coefficients on afterburning rocket plumes. *J. Spacecraft Rockets*, 8, p. 643.
- Rhodes, R.P. (1977). Preliminary gas dynamic analysis of rocket plumes for subsonic and supersonic external air flows. *AEDC-TR-76-137*, Arnold Engineering Development Center, Arnold Air Force Station, TN.

Rhodes, R.P., Harsha, P.T., and Peters, C.E. (1974). Turbulent kinetic energy analyses of hydrogen-air diffusion flames. *Acta Astronautica*, Vol. 1, pp. 443-470.

Rodi, W., and Spalding, D.B. (1970). A two-parameter model of turbulence and its application to free jets. *Wärme - und Stoffübertragung*, Springer-Verlag, Vol. 3, Berlin, pp. 85-95.

Smoot, L.D. (1976). Turbulent mixing coefficients for compressible coaxial submerged and coflowing jets. *AIAA J.*, Vol. 14, No. 12, pp. 1699-1705.

TABLE I. H_2/O_2 COMBUSTION REACTIONS

REACTION	RATE COEFFICIENT (molecule-cm-sec units)	
	PRESENT VALUES	NEW RECOMMENDED VALUES ^a
A1 $H + OH + M \rightarrow H_2O + M$	$1.4 \times 10^{-29} T^{-1}$	$1.0 \times 10^{-25} T^{-2}$
A2 $O + H + M \rightarrow OH + M$	$1.0 \times 10^{-29} T^{-1}$	3.0×10^{-32}
A3 $O + O + M \rightarrow O_2 + M$	b	$5.0 \times 10^{-30} T^{-1} \exp(-340/RT)$
A4 $H + H + M \rightarrow H_2 + M$	$1.0 \times 10^{-29} T^{-1}$	$5.0 \times 10^{-30} T^{-1}$
B1 $OH + H \rightarrow H_2 + O$	$1.3 \times 10^{-11} \exp(-7380/RT)$	$1.4 \times 10^{-14} T \exp(-7000/RT)$
B2 $OH + O \rightarrow H + O_2$	$3.0 \times 10^{-11} \exp(-860/RT)$	4.0×10^{-11}
B3 $OH + H_2 \rightarrow H_2O + H$	$3.6 \times 10^{-11} \exp(-5200/RT)$	$1.0 \times 10^{-17} T^2 \exp(-2900/RT)$
B4 $OH + OH \rightarrow H_2O + O$	$9.7 \times 10^{-12} \exp(-1660/RT)$	$1.0 \times 10^{-11} \exp(-1100/RT)$

^a See Appendix for sources of rate coefficient data.

^b Not used in present calculations.

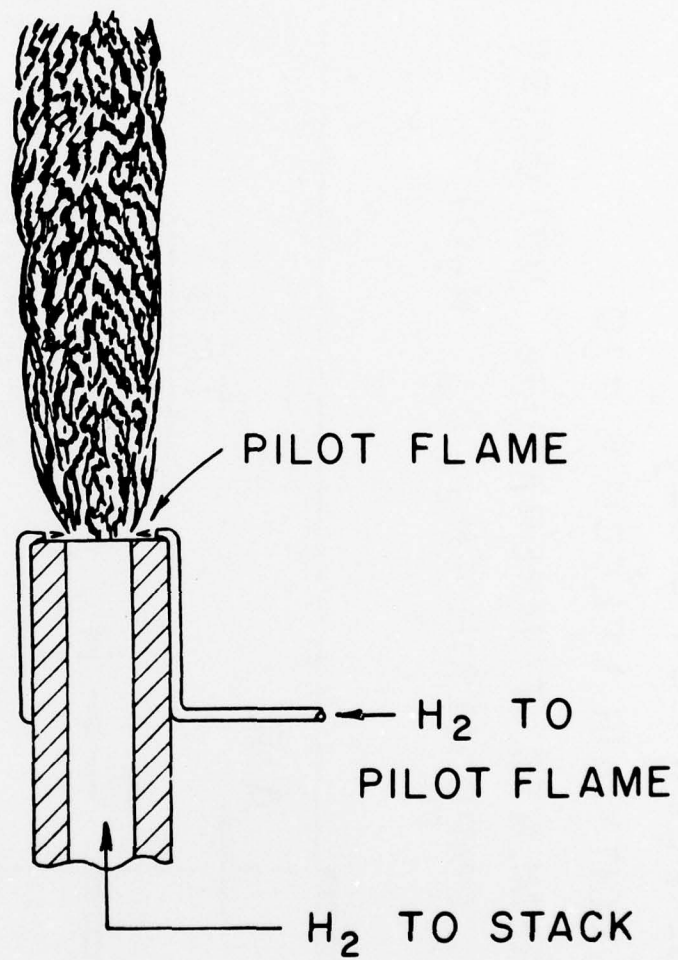


Figure 1. H₂/air diffusion flame with pilot ignition.

H₂ NOZZLE DIAMETER = .76 CM

H₂ MASS FLOW = .54 G/SEC

H₂ VELOCITY/AIR VELOCITY ≈ 10

MEASUREMENTS: TEMPERATURE, VELOCITY &

COMPOSITION (H₂, O₂, H₂O)

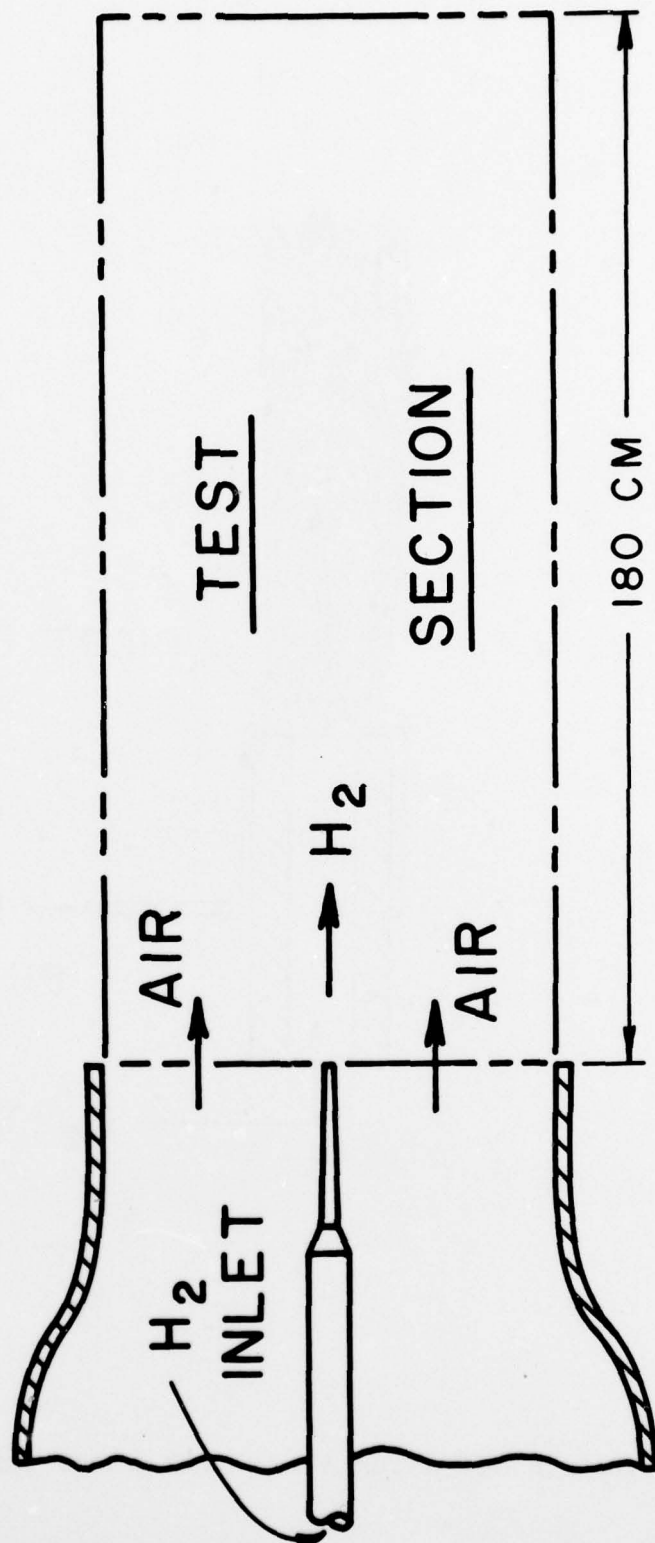


Figure 2. Experimental setup of Kent and Bilger (1973).

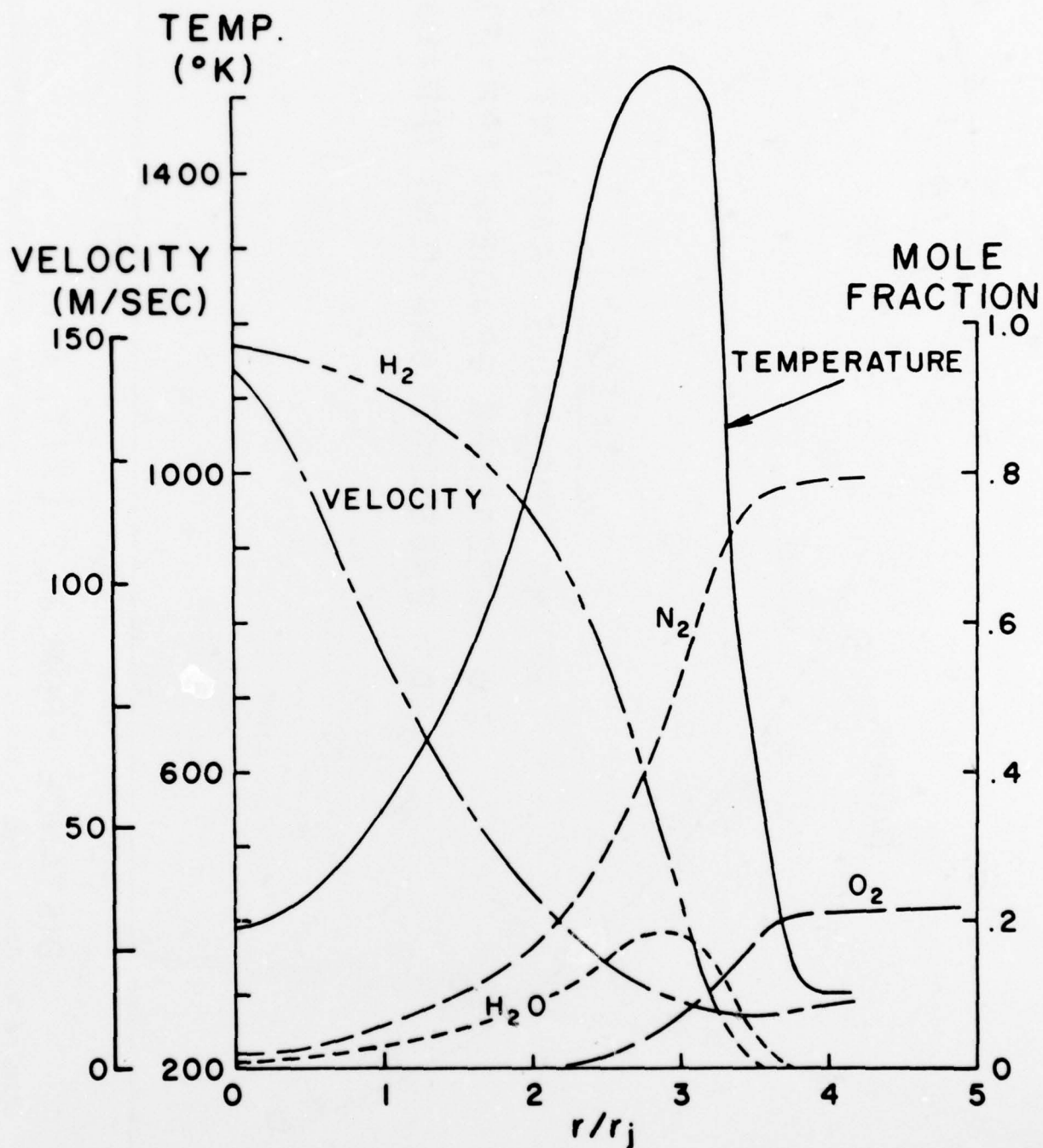


Figure 3. Initial conditions for model predictions to compare with data of Kent and Bilger (1973); $x/r_j = 12.2$.

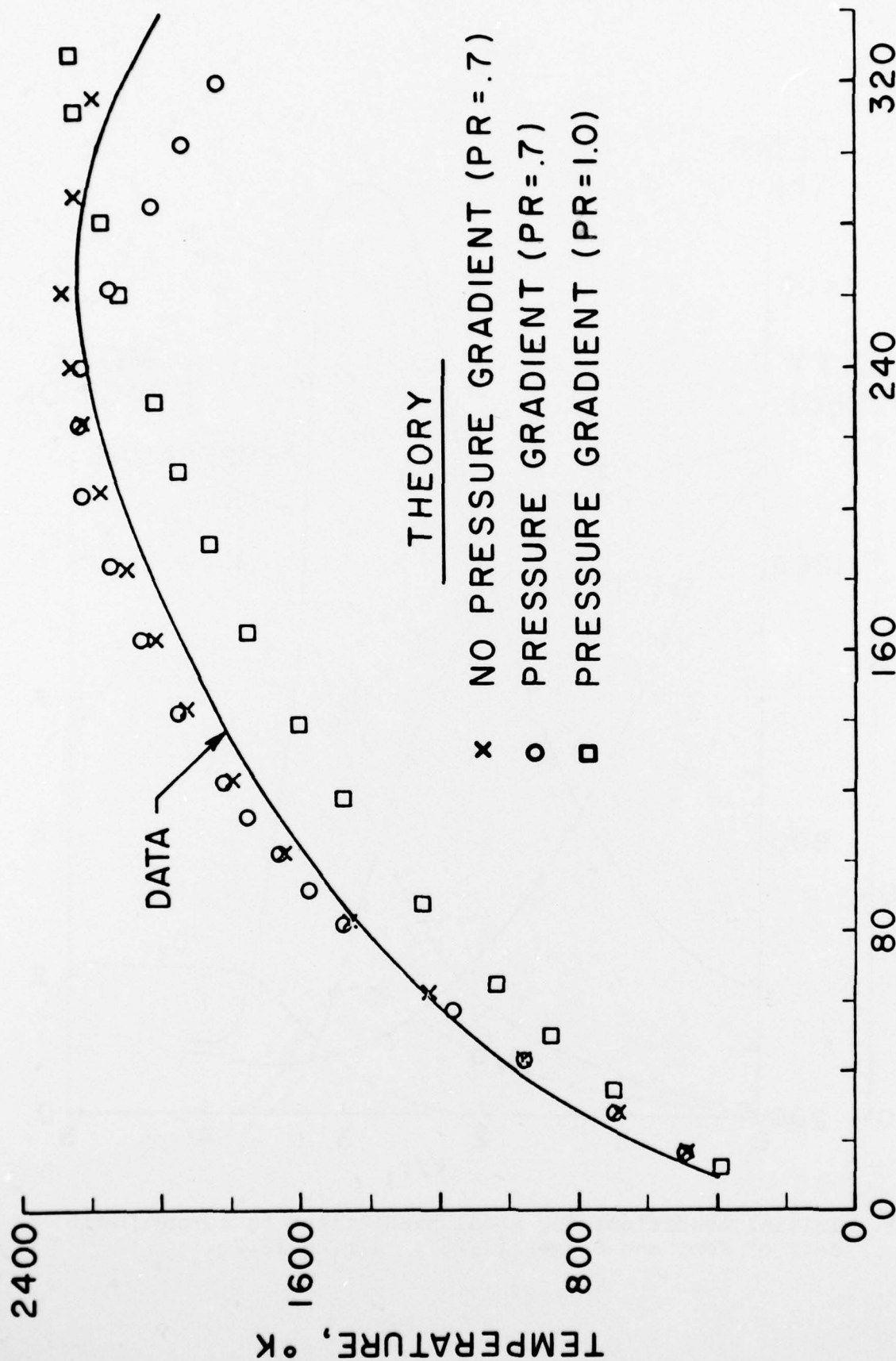


Figure 4. Comparison between predicted and measured centerline temperatures H_2 /air laboratory flame, $r_j = 0.38$ cm.

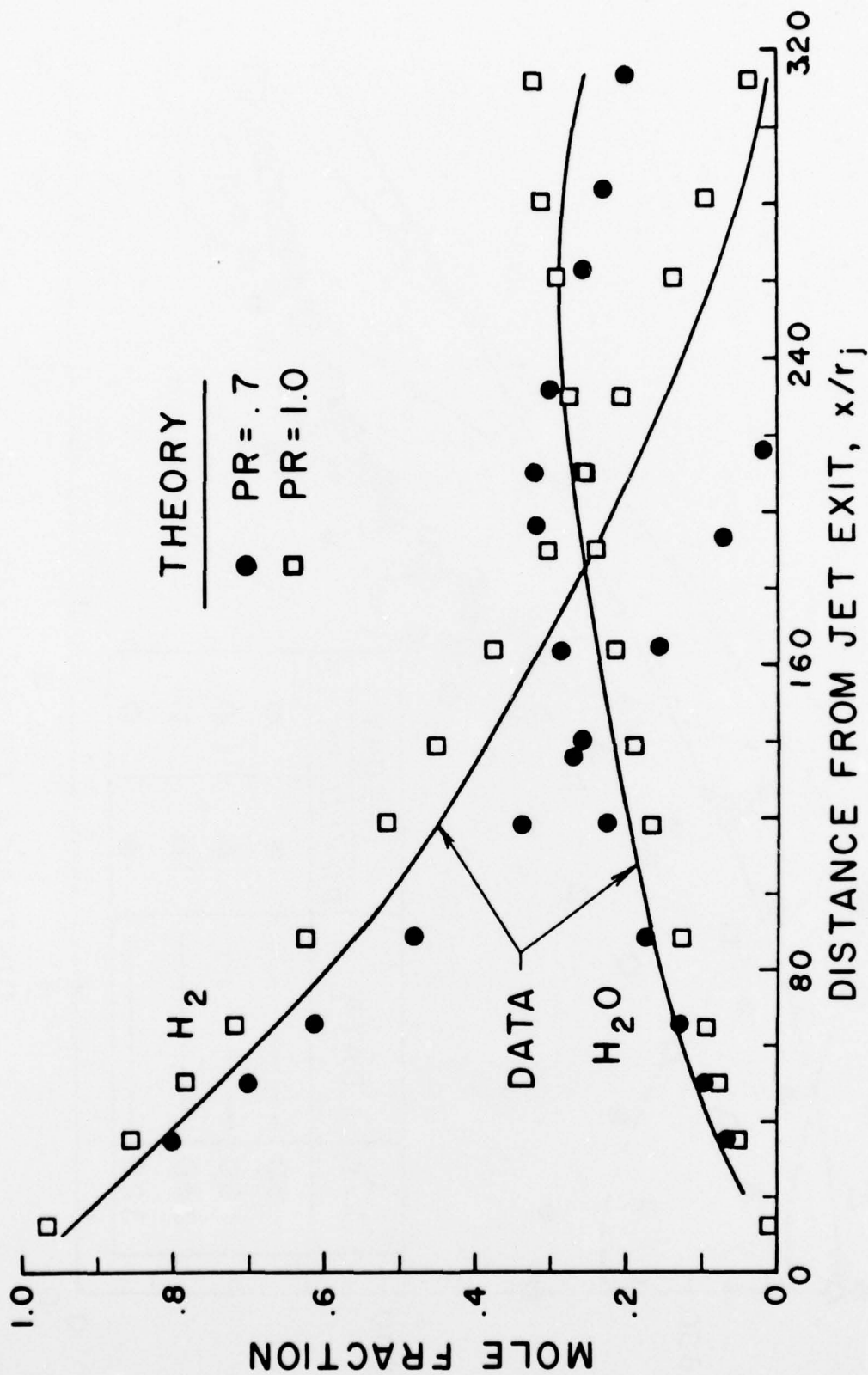


Figure 5. Comparison between predicted and measured centerline mole fractions- H_2 /air laboratory flame, $r_j = 0.38$ cm .

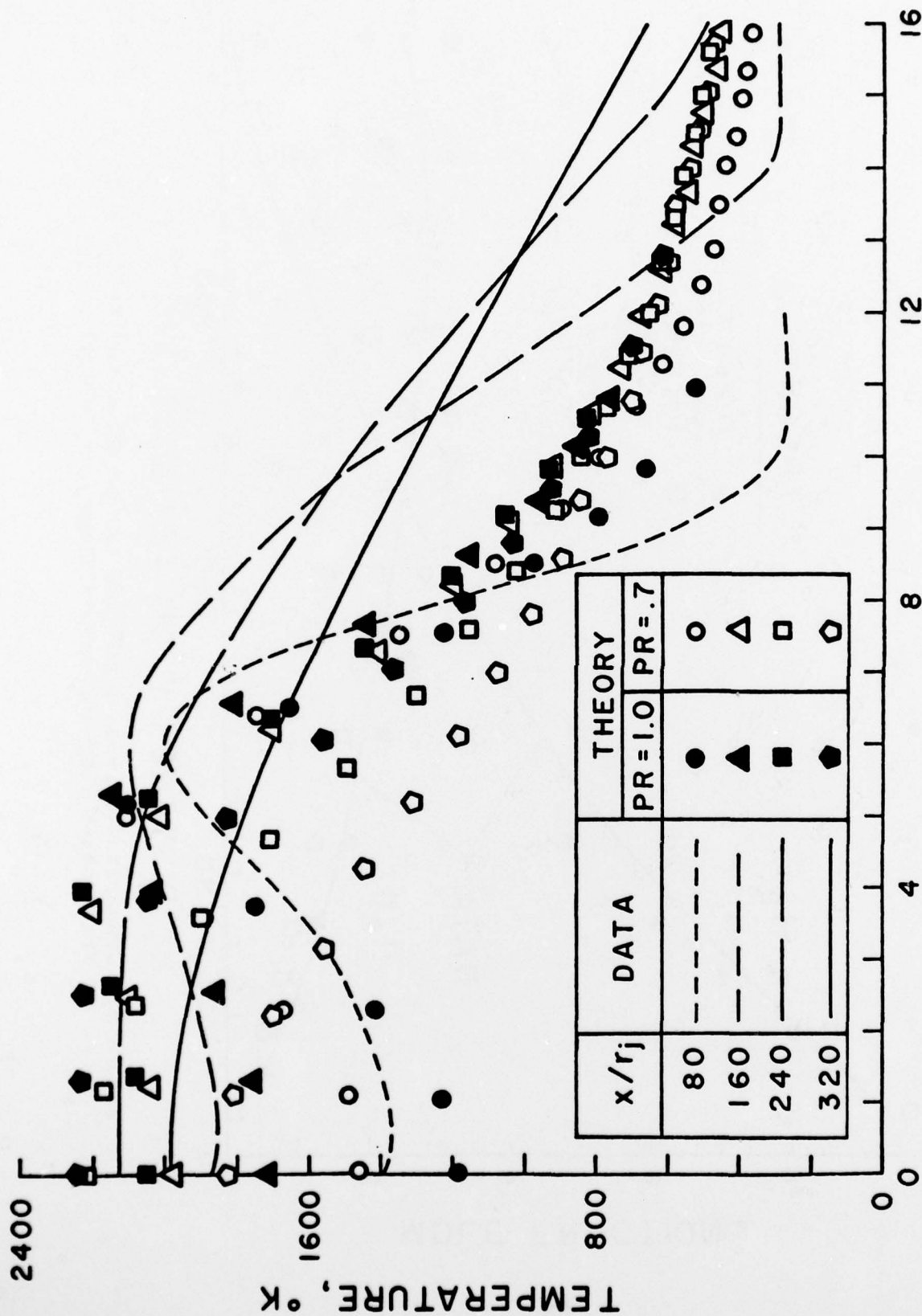


Figure 6. Comparison between predicted and measured radial temperature profiles-H₂/air laboratory flame, $r_j = 0.38$ cm.

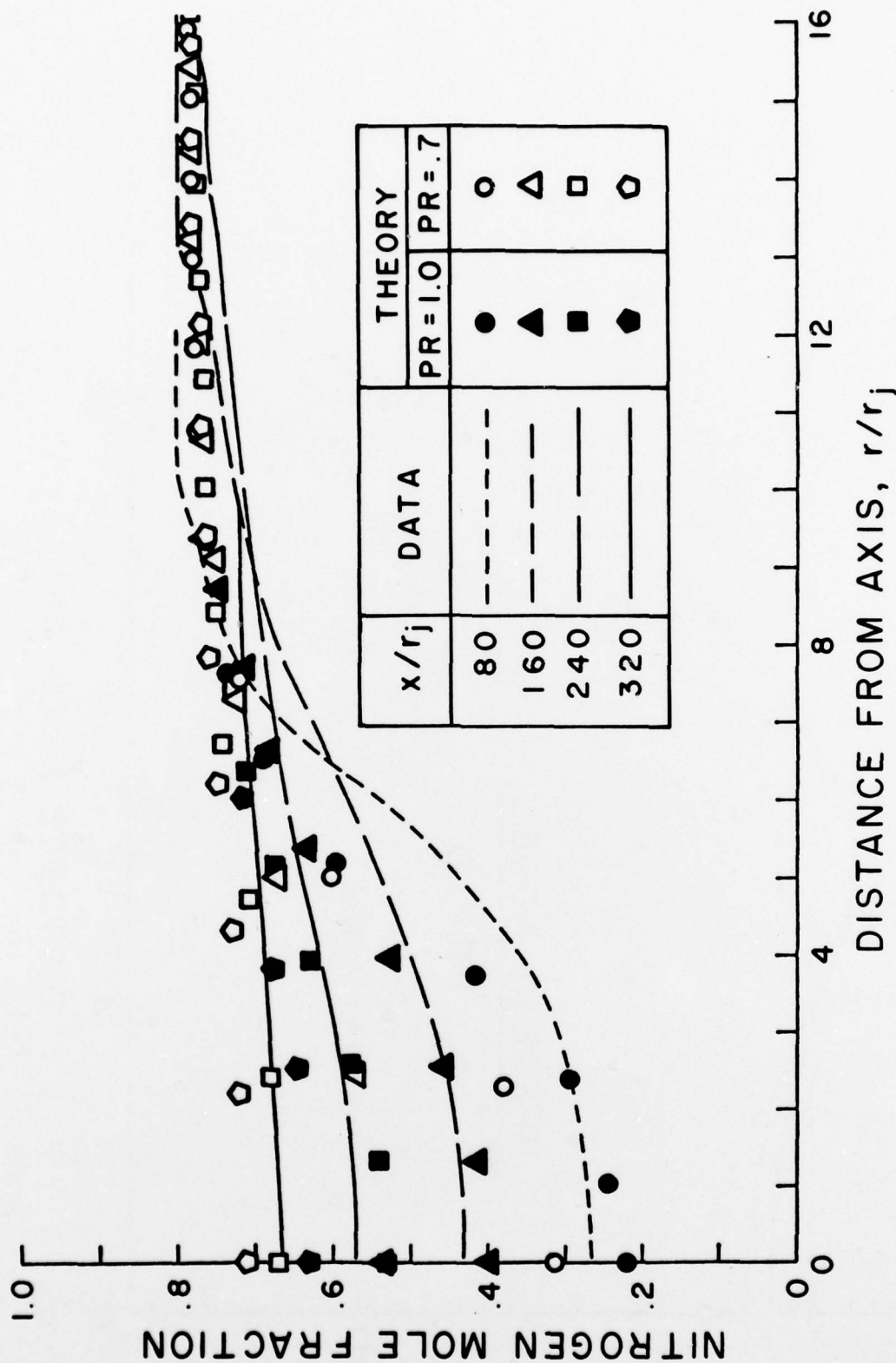


Figure 7. Comparison between predicted and measured radial nitrogen mole fraction profiles- H_2 /air laboratory flame, $r_j = 0.38$ cm .

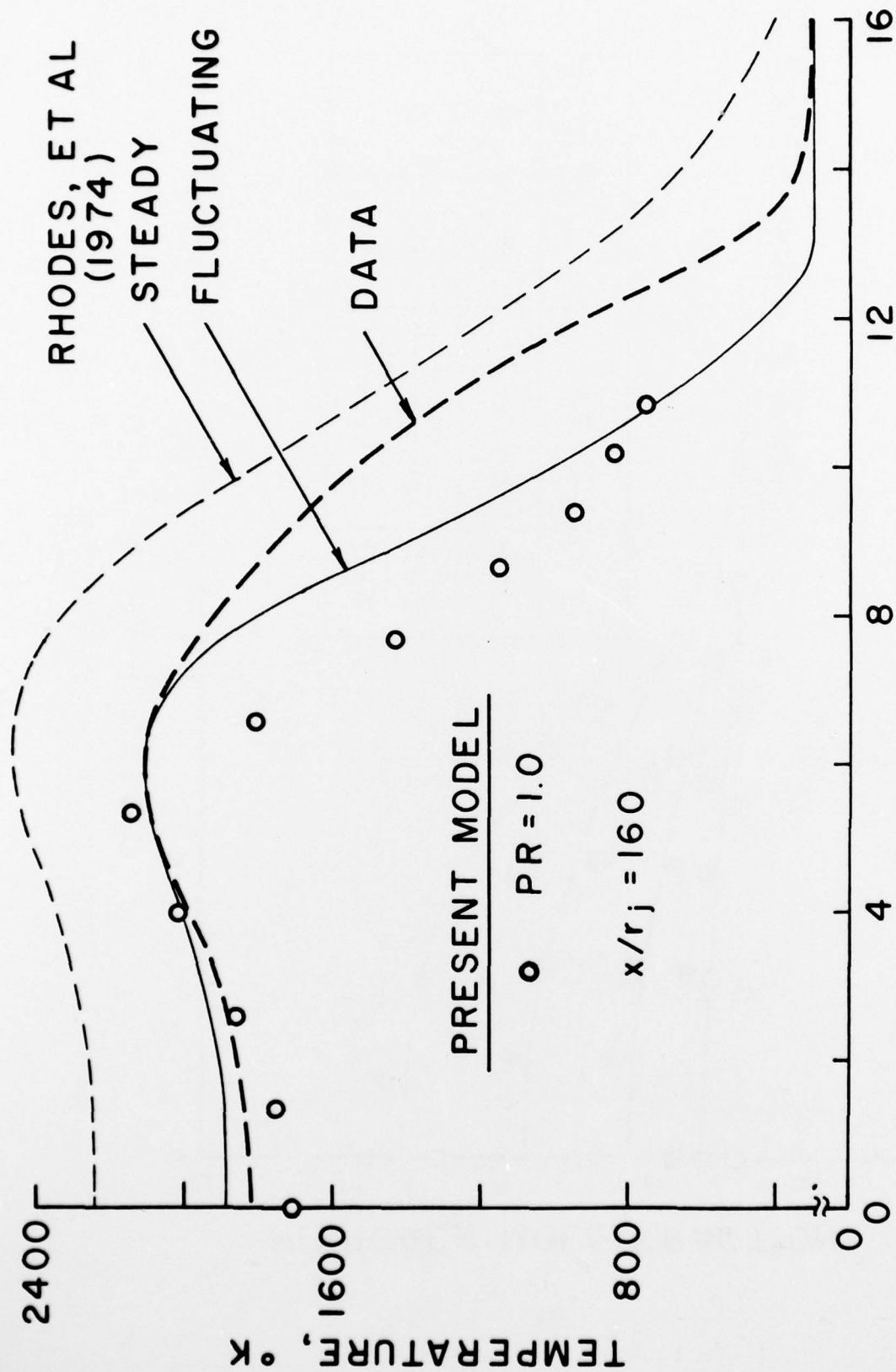


Figure 8a. Comparison between temperature profiles predicted by present model and Rhodes et al. (1974); $x/r_j = 160$.

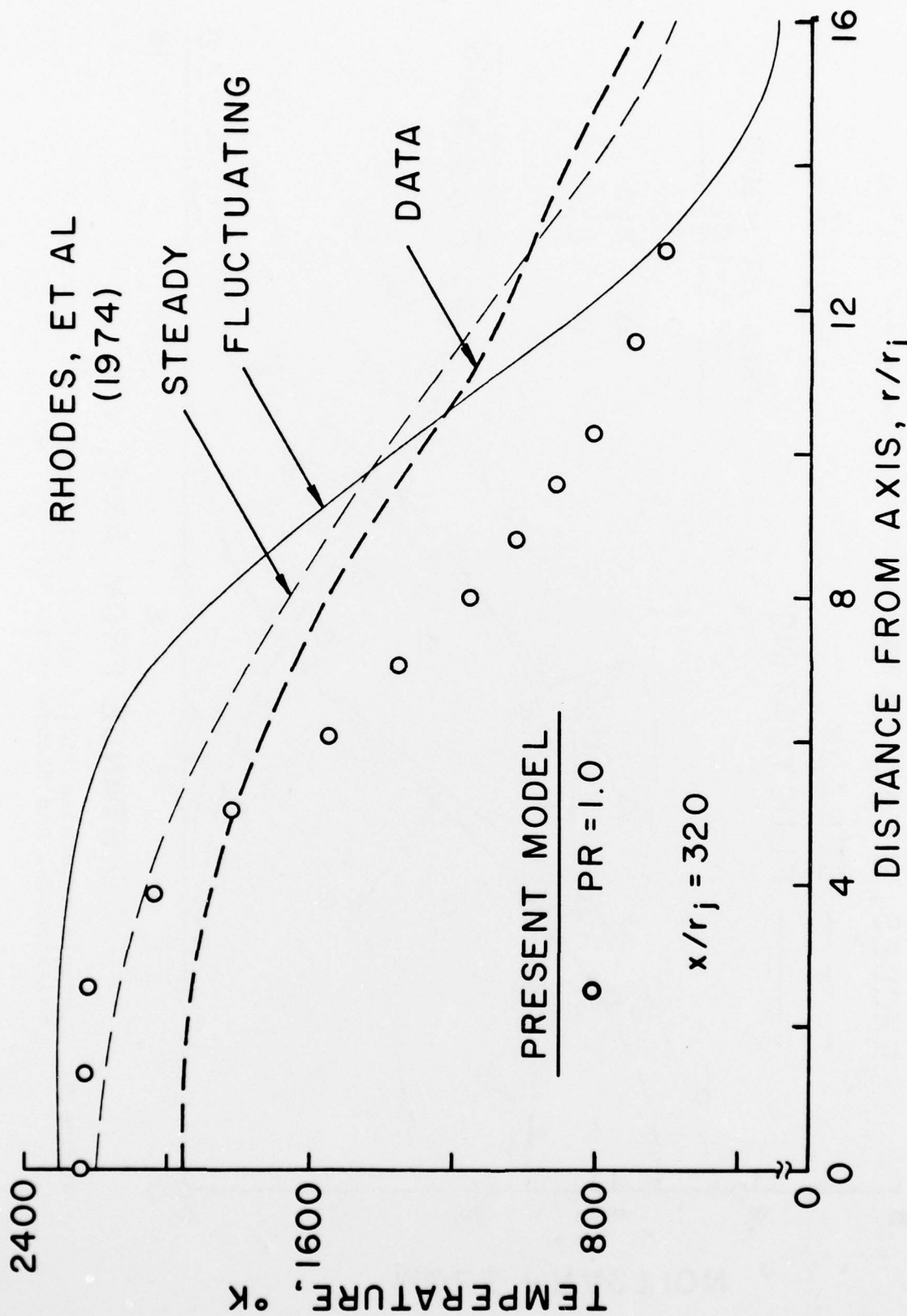


Figure 8b. Comparison between radial temperature profiles predicted by present model and Rhodes et al. (1974); $x/r_j = 320$.

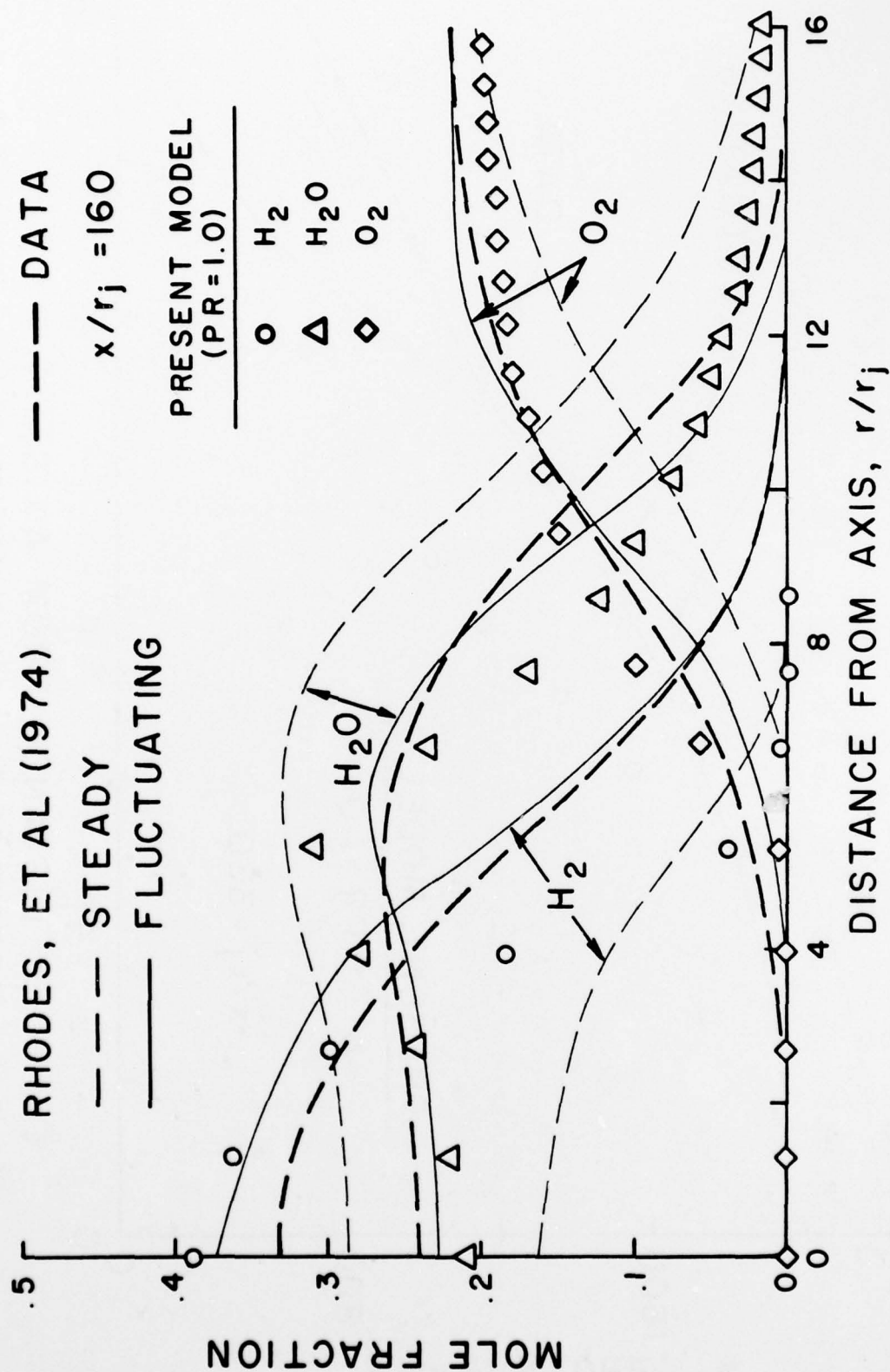


Figure 9. Comparison between radial mole fraction profiles predicted by present model and Rhodes et al. (1974); $x/r_j = 160$.

A.R.A.P. RSL CODE
 FISHBURNE, ET AL (1977)
 --- 'LAMINAR' CHEM.
 — 'TURBULENT' CHEM.
 --- EXPERIMENTAL
 DATA

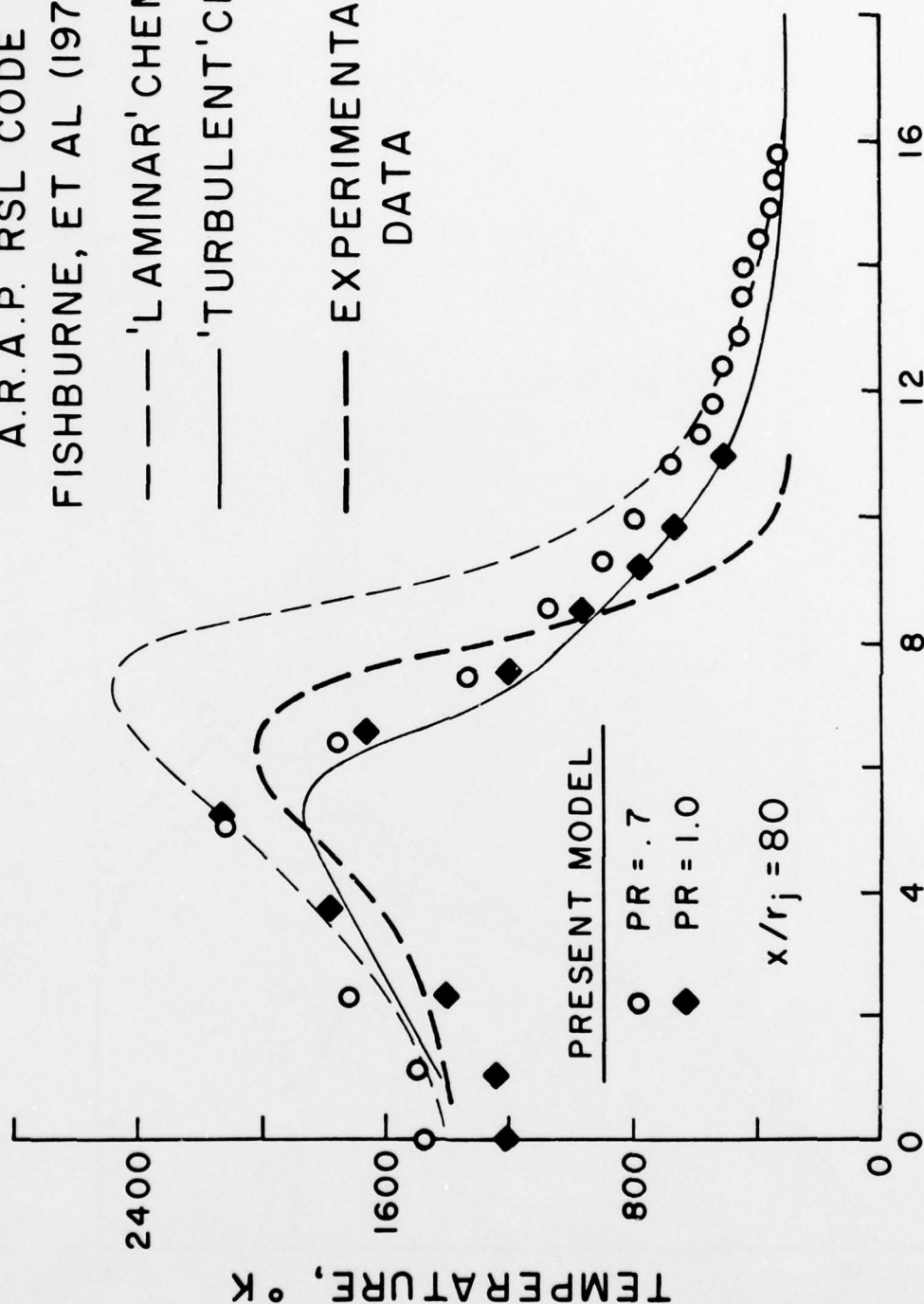


Figure 10. Comparison between radial temperature profiles predicted by present model and second-order closure model of Fishburne et al. (1977); $x/r_j = 80$.

A.R.A.P. RSL CODE
FISHBURNE, ET AL (1977)

--- 'LAMINAR' CHEM.

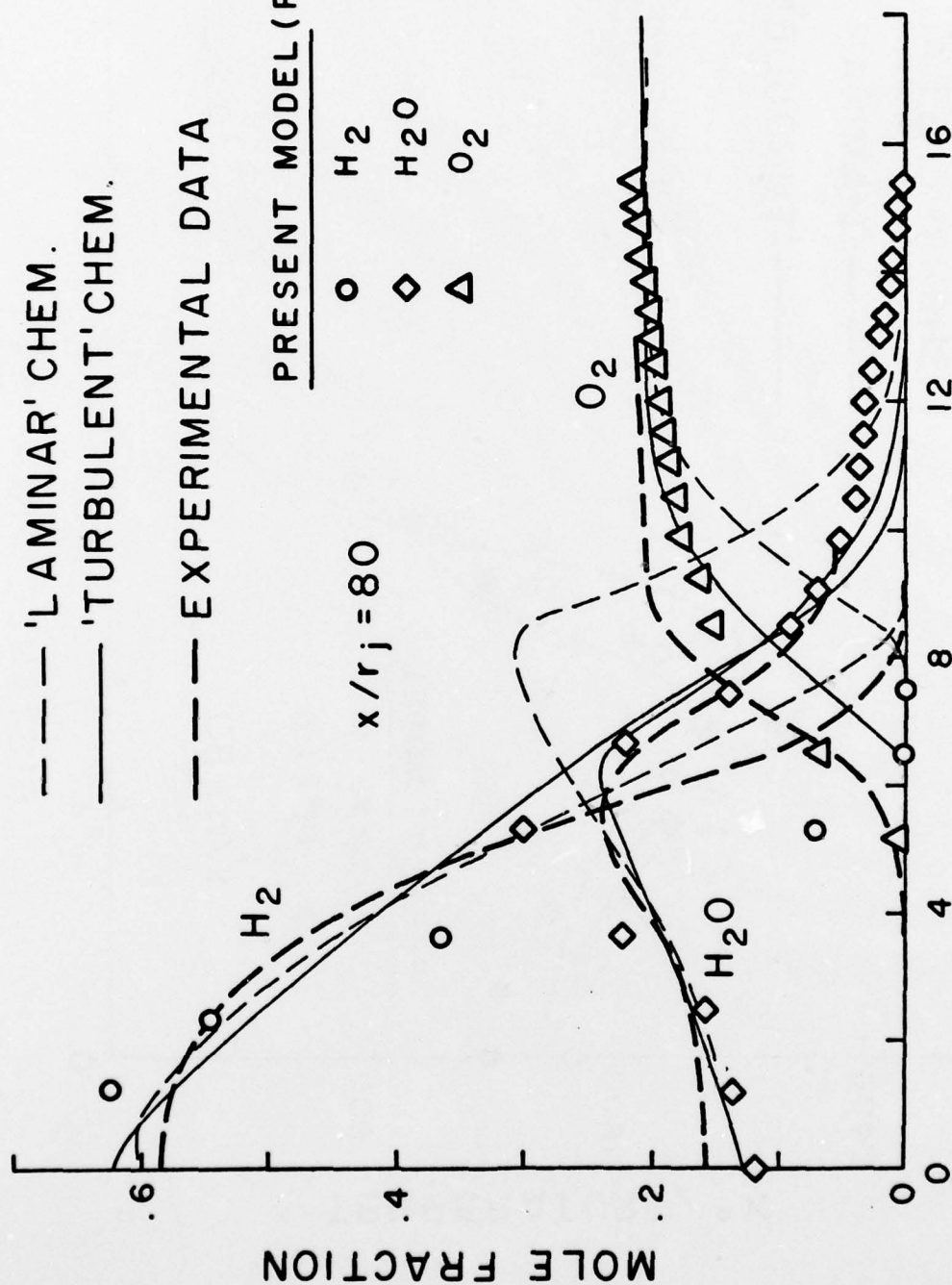
— 'TURBULENT' CHEM.

--- EXPERIMENTAL DATA

PRESENT MODEL (PR=1.0)

○	H ₂
◇	H ₂ O
△	O ₂

$x/r_j = 80$



Distance from Axis, r/r_j

Figure 11. Comparison between radial mole fraction profiles predicted by present model and second-order closure model of Fishburne et al. (1977); $x/r_j = 80$.

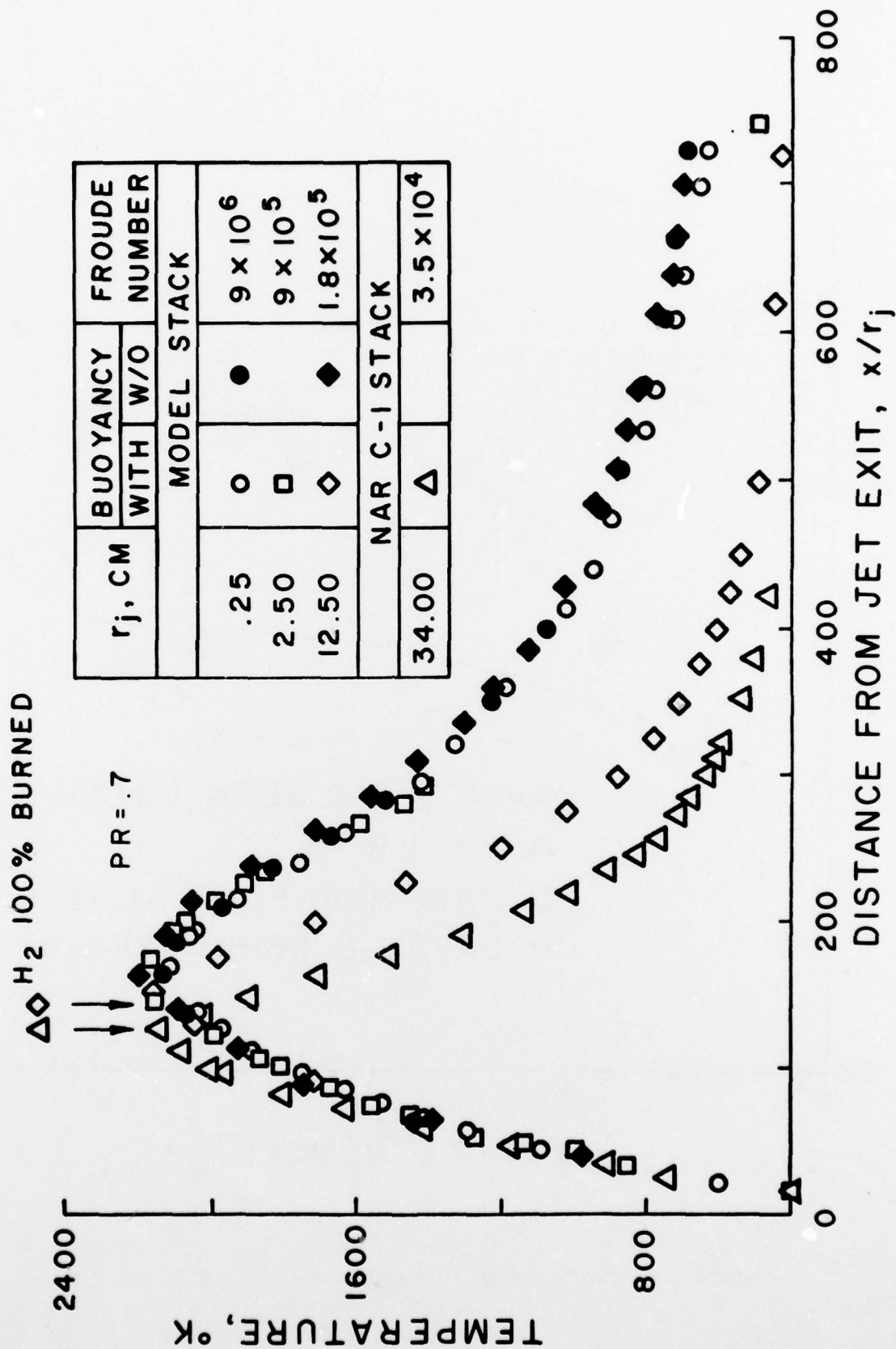


Figure 12. Influence of buoyancy on H₂/air flame centerline temperatures.

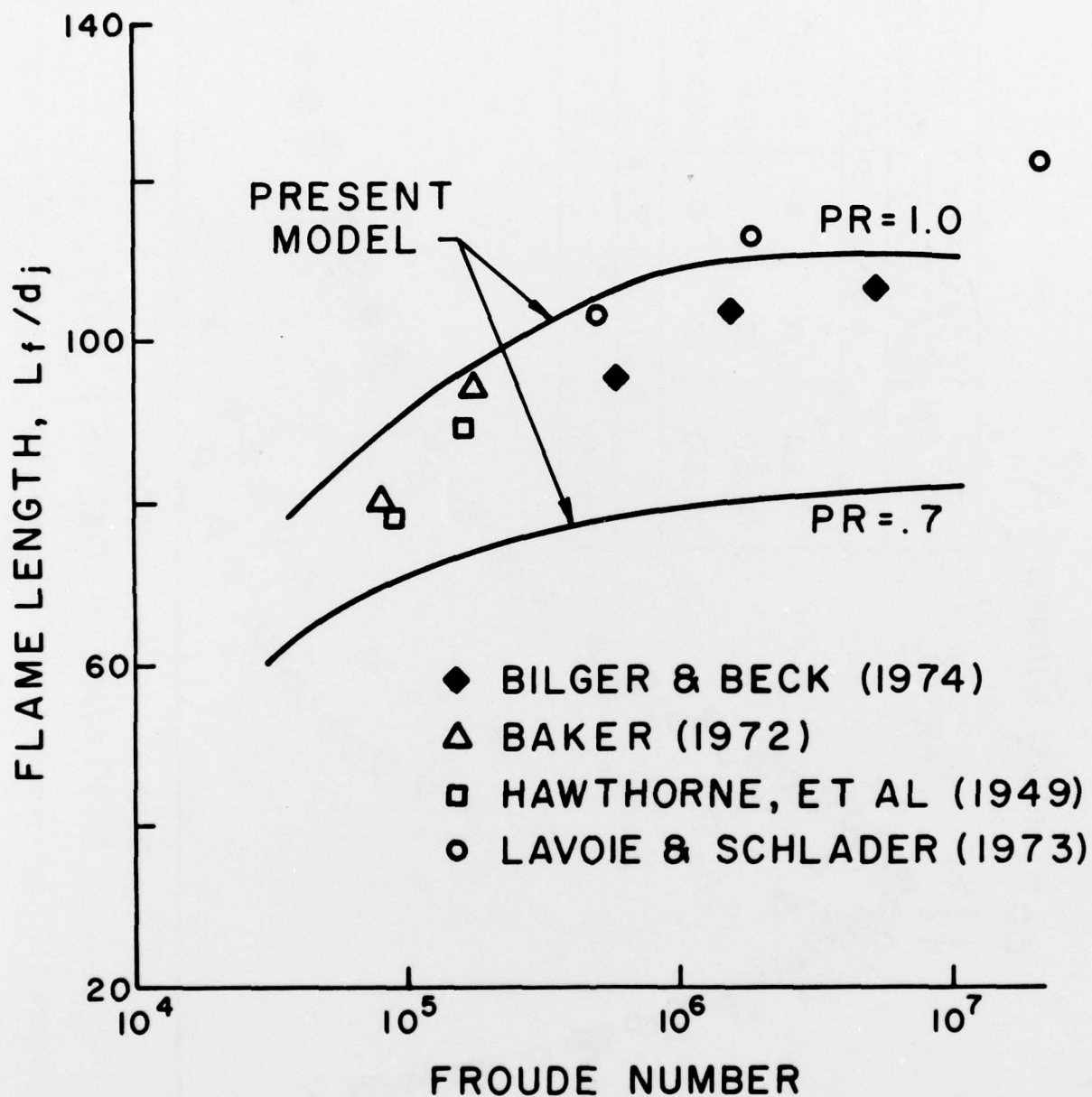


Figure 13. Influence of Froude number on flame length.